Journal of Alloys and Compounds 509 (2011) 8116–8119

Contents lists available at ScienceDirect

Journal of Alloys and Compounds

journal homepage: www.elsevier.com/locate/jallcom

Infrared emissivity of Sr doped lanthanum manganites in coating form

Xingmei Shen[a,*], Liaosha Li[a], Xingrong Wu[a], Zhifang Gao[a], Guoyue Xu[b]

[a] Anhui Provincial Key Laboratory of Metallurgy Engineering & Resources Recycling, Anhui University of Technology, Ma'anshan, Anhui Province 243002, China
[b] College of Material Science & Engineering, Nanjing University of Aeronautics and Astronautics, Yu Dao Street 29, Nanjing 210016, China

ARTICLE INFO

Article history:
Received 19 February 2011
Received in revised form 18 May 2011
Accepted 18 May 2011
Available online 27 May 2011

Keywords:
Ceramics
Solid state reaction
Optical properties
Light absorption and reflection

ABSTRACT

The Sr doped lanthanum manganite coatings were prepared using $La_{0.8}Sr_{0.2}MnO_3$ particles and epoxy modified polyurethane as pigment and resin matrix, respectively. The structure, morphology, surface roughness and infrared normal emissivity (ε_N) in the 3–5 and 8–14 μm wavebands of the samples were systematically investigated. With the increase of $La_{0.8}Sr_{0.2}MnO_3$ pigment, the ε_N of the coatings decreases and the ε_N values in the 8–14 μm waveband are higher than those in the 3–5 μm waveband. The surface roughness has no significant effect on the infrared emissivity of LSMO coatings. For 50% LSMO coating, the sample shows variable-emissivity property in the 8–14 μm waveband and the emissivity property remains unchanged before and after ultraviolet irradiation.

1. Introduction

As we know, infrared emissivity (ε) is an important factor for electromagnetic radiation. Higher emissivity can lead to higher radiation energy. Thus, infrared emissivity of some materials is expected to change with temperature to fulfill certain requirements, which is called variable-emissivity materials. For example, emissivity of materials for military aircraft is needed to decrease with increasing temperature, which could decrease the radiation energy to achieve thermal stealth. Emissivity of materials for satellites is expected to increase with increasing temperature to perform autonomous thermal control [1–3], and emissivity of materials for buildings is also desired to increase with increasing temperature [4]. Owing to these unique thermal control applications, variable-emissivity materials have attracted much attention and are of great significance for national defence and energy conservation. However, the variable-emissivity materials in use now must be electrified or need some accessories to be installed [5–10]. Then, they are inapplicable in several cases, which limits their applications.

It has been reported that doped manganites at certain doping levels undergo metal–insulator (MI) phase transition [11–13], and even two MI transition peaks were observed in several doped manganites [14]. The above mentioned phenomenon has been explained by means of double-exchange interaction between Mn^{3+} and Mn^{4+}, and electron–phonon interaction relating to Jahn–Teller-type lattice distortion of the MnO_6 octahedra [15–17]. In general, emissivity of metal is low, while that of insulator is high, and IR emissivity has been used as a potent tool to characterize metal–insulator transition [18]. Thus, without electricity or any accessories, the emissivity of doped manganites can change significantly with temperature due to MI phase transition, which makes them attractive as autonomous thermal control material. Previous works have mainly focused on infrared emissivity of doped manganites in bulk form rather than coating form. K. Shimazaki et al. [19] have reported that, in the vicinity of $x = 0.2$ Sr doping level, bulk Sr-doped lanthanum manganites showed remarkable emissivity variation and the infrared spectral reflectance was studied to investigate the influence of Sr doping on the emissivity. Temperature-dependent emissivity properties of bulk Sr-doped lanthanum manganites were studied by G. Tang et al. [20–22], which were explained by electrical resistivity and infrared reflection results, and C. Wu et al. [23] have reported that variable emissivity property also exists in Sr-doped lanthanum manganite thin films by magnetron sputtering. Then, what about the infrared emissivity of $La_{1-x}Sr_xMnO_3$ in coating form, which may have potential application for buildings? However, studies on the emissivity of $La_{1-x}Sr_xMnO_3$ coating have not been reported yet.

Therefore, this work is focused on the infrared emissivity of $La_{1-x}Sr_xMnO_3$ coating and $x = 0.2$ Sr doped lanthanum manganites (LSMO), which exhibits the greatest emissivity variation, is chosen as the pigment.

2. Experimental procedures

LSMO pigment: La_2O_3, $SrCO_3$ and MnO_2 were used as raw materials and La_2O_3 was fired in air at 1173 K for 7 h before use. Ethanol was added as a milling medium

* Corresponding author. Tel.: +86 555 2311879; fax: +86 555 2311879.
E-mail address: xxxxmx@126.com (X. Shen).

0925-8388/$ – see front matter © 2011 Elsevier B.V. All rights reserved.
doi:10.1016/j.jallcom.2011.05.072

together with the raw materials. After milling for 12 h, the mixture was air-dried at 353 K to remove the ethanol and calcined at 1273 K, and finally sintered at 1473 K for 24 h.

LSMO coatings: tinplate substrates were cleaned by 10% dilute H_2SO_4 and deionized water, respectively before use. Above prepared LSMO particles and epoxy modified polyurethane were used as pigment and resin matrix, respectively. Coupling agent and hardening agent were added under continuous ultrasonication for 30 min. Then the mixture was coated on tinplate substrates using a paint roller, and the thickness of the coatings was about 100 μm. The coatings were dried in an oven at 353 K for 48 h. Finally, the coatings were dried at room temperature for 7 days.

The structure of LSMO was characterized by Bruker D8 X-ray powder diffraction (XRD) using Cu Kα radiation (λ = 0.15405 nm) operated at 40 kV and 40 mA. The morphology of the coatings was observed by FEI-Quanta200 scanning electron microscope (SEM). The surface roughness was observed by a Mahr perthometer S3P instrument (Germany), and the standard instrumental error of the instrument is ±0.1 μm. The infrared normal emissivity (ε_N) in the 3–5 and 8–14 μm wavebands, respectively, was measured from 288 K to 373 K by the IR-2 infrared emissometer (Shanghai Institute of Technological Physics, China) with the blackbody temperature 623 K and 523 K. The emissivity of Al-plate corrector and Cu-plate corrector is 0.05 and 0.5, respectively, and the measurement error of ε_N is less than 0.001. The ultraviolet irradiation test was performed under 302 nm ultraviolet lamp.

3. Results and discussion

Fig. 1 shows the XRD pattern of LSMO sample. As can be seen from the figure, the sample is single phase exhibiting characteristic peaks of the perovskite structure. The separation of peaks at 32.6°, 40.3°, 58.3°, 68.4° and 77.8° indicates that the sample is rhombohedral with space group R-3c (JCPDS Card, No. 53-0058).

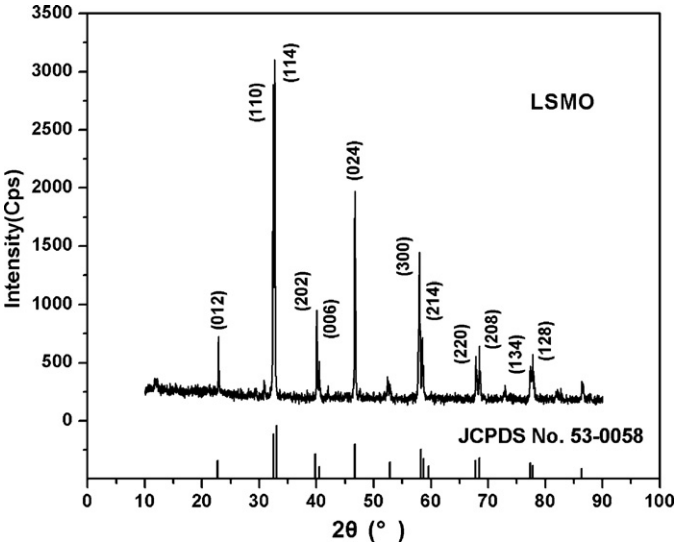

Fig. 1. The XRD pattern of LSMO sample.

The SEM images of 10% and 50% LSMO coatings are shown in Fig. 2(a) and (b), respectively. As can be seen in the figure, the prepared LSMO particles are 1–2 μm. For 10% LSMO coating, the particles are dispersed evenly in the coating. For 50% LSMO coating, the particles are closely attached to each other. Emissivity values of 50% LSMO coating with different surface roughness are shown in Table 1. From the table, it can be seen that emissivity of the samples in both 3–5 and 8–14 μm wavebands has no obvious change with surface roughness. When a beam of electromagnetic radiation is incident on an interface, some of the radiations are reflected and

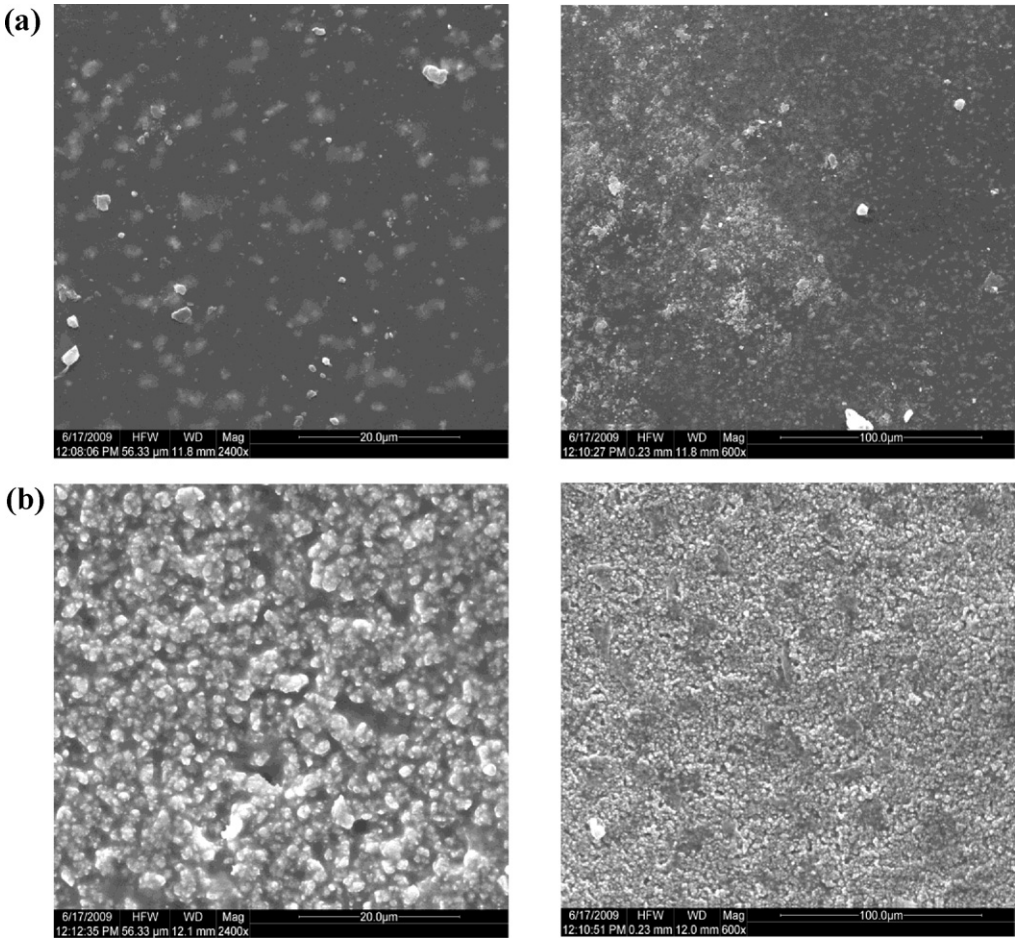

Fig. 2. (a) The SEM images of 10% LSMO ($x = 0.2$) coating. (b) The SEM images of 50% LSMO ($x = 0.2$) coating.

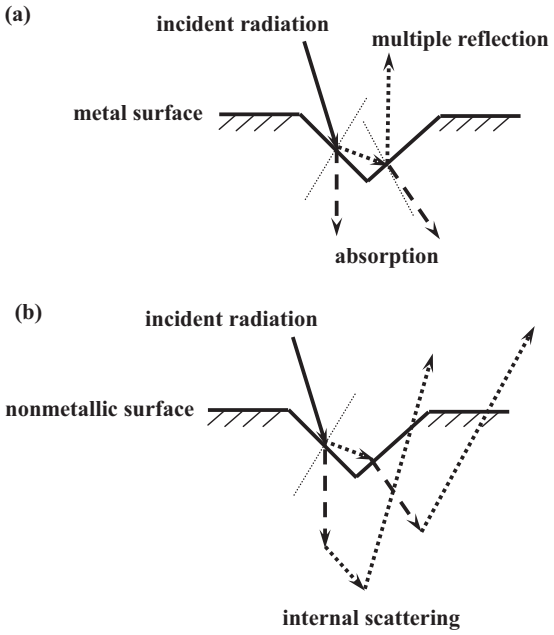

Fig. 3. Schematic diagram of electromagnetic radiation acting on different surfaces.

some of the radiations are refracted into sample. For metallic pigment, reflection, absorption and emission occur only at the thin surface. With increasing surface roughness, multiple reflections occur at the uneven surface and absorption probability increases as shown in Fig. 3(a), which results in the increase of emissivity. Thus, surface roughness has great effect on the emissivity of metals. However, for LSMO polycrystalline pigment with particle size (1–2 μm) less than the wavelength, emissivity of the coating is determined by volumetric absorption and scattering properties. The absorption coefficient is usually weakly sensitive to the material morphology and it is determined by chemical composition and porosity of the material. On the contrary, the effective scattering coefficient is determined by the coating substance refractive index and especially by morphology of the dispersed coating [24]. Due to the higher internal scattering, the radiation inside the surface, induced by increased surface roughness, finally returns to the surface, as shown in Fig. 3(b). Therefore, the surface roughness has no significant effect on the emissivity. From Table 1, it can be seen that ε_N of the samples in the 3–5 and 8–14 μm wavebands is about 0.65 and 0.86, respectively, and has no obvious change with surface roughness.

Table 1
The ε_N values of LSMO coating with different surface roughness.

Surface roughness	1.3 μm	1.8 μm	2.1 μm
ε_N in the 3–5 μm waveband	0.657	0.658	0.658
ε_N in the 8–14 μm waveband	0.862	0.861	0.862

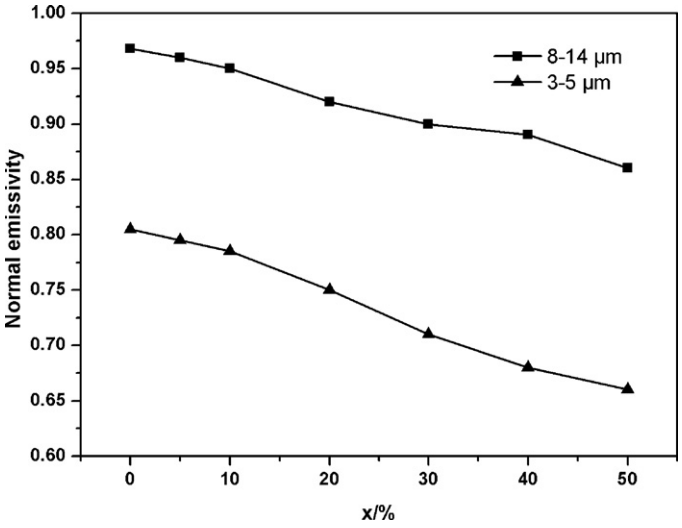

Fig. 4. The relationship between the ε_N of the coatings and LSMO concentration in both 3–5 and 8–14 μm wavebands.

Fig. 4 shows the relationship between the ε_N of the coatings and LSMO concentration in both 3–5 and 8–14 μm wavebands. As can be seen in the figure, ε_N of the coatings decreases with increasing LSMO, and ε_N of $x = 100\%$ sample in the 8–14 μm waveband decreases to 0.693, which was reported in our previous work [25]. The reason for this can be explained by Fig. 5. The resin matrix usually possesses higher emissivity value due to intense absorption in the infrared waveband. When the concentration of LSMO is low, the particles are dispersed evenly in the resin matrix, thus, epoxy modified polyurethane absorbs large amounts of radiation, as shown in Fig. 5(a), which results in high emissivity of the coatings. With the increase of LSMO concentration, the particles are closely attached to each other, then, the particles reflect large amounts of radiation as shown in Fig. 5(b), and increased reflectivity results in the decrease of emissivity. Note that ε_N of the coatings in the 8–14 μm waveband is higher than that in the 3–5 μm waveband. According to Planck law, $E = h\nu = hc/\lambda$ (h is Planck constant), photon energy is inversely proportional to waveband. Then, photon energy in the 8–14 μm waveband is lower than that in the 3–5 μm waveband,

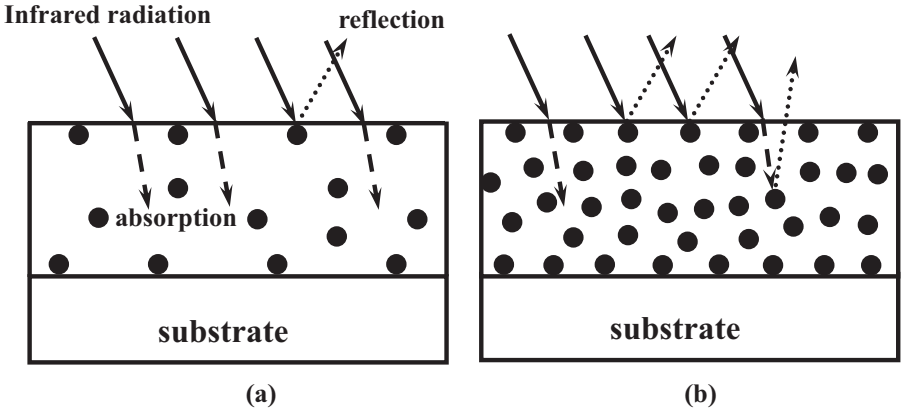

Fig. 5. Schematic diagram of electromagnetic radiation acting on different coatings.

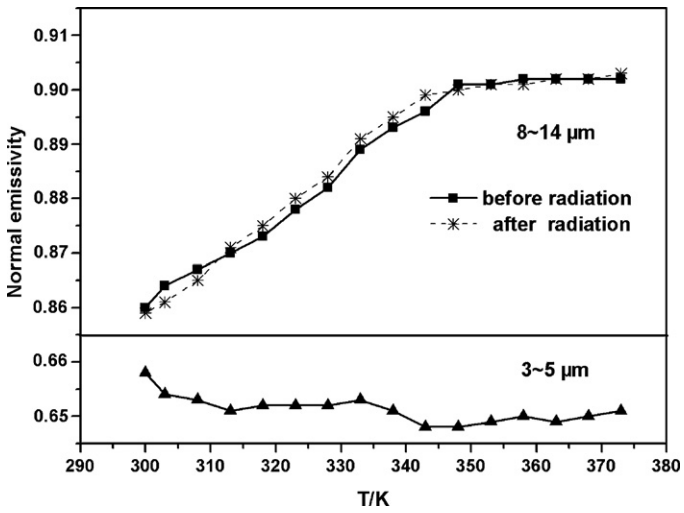

Fig. 6. The temperature dependence of the ε_N of 50% LSMO coating in both 3–5 and 8–14 μm wavebands (before and after ultraviolet irradiation).

Table 2
The ε_N values of 50% LSMO coating under different ultraviolet irradiation time.

Ultraviolet irradiation time/day	1	7	14	30
ε_N	0.860	0.859	0.860	0.859

and optical excitation energy for emission in the 8–14 μm waveband is lower, which means that the emission probability is higher. Therefore, the emissivity in the 8–14 μm waveband is higher.

Fig. 6 shows the temperature dependence of the ε_N of 50% LSMO coating in both 3–5 and 8–14 μm wavebands. From the figure, it can be seen that 50% LSMO coating shows variable-emissivity property in the 8–14 μm waveband and no drastic change occurs in the 3–5 μm waveband. According to Wien's displacement law $\lambda_m T = b$ (λ_m is the wavelength at which the radiated power is maximum, T is temperature, b is Wien's displacement constant and $b = 2897.8 \pm 0.4$ μm K), λ_m is inversely proportional to temperature, and temperature corresponding to 3–5 μm waveband is at 580–965 K, indicating that most high-energy atoms in the 3–5 μm waveband are in the temperature range of 580–965 K, but fewer in the temperature range of 280–380 K. Thus, the ε_N of the sample in the 3–5 μm waveband is lower exhibiting metallic character at 280–380 K, and increases gradually with temperature. In the 8–14 μm waveband, temperature for most high-energy atoms is just at 280–380 K, and this is another reason for higher emissivity value in the 8–14 μm waveband at room temperature. Table 2 shows the ε_N of 50% LSMO coating under different ultraviolet irradiation time. From the table, it can be seen that the ε_N remains constant after 30 days of ultraviolet irradiation, and no obvious damage or change occurs on the coating. The temperature dependence of the ε_N of 50% LSMO coating after ultraviolet irradiation is also shown as a dotted line in Fig. 6. It is clear that the LSMO coating shows variable-emissivity property, and emissivity property remains unchanged before and after ultraviolet irradiation.

4. Conclusions

In summary, the infrared emissivity of Sr doped lanthanum manganite coatings decreases with LSMO concentration, and the emissivity values in the 8–14 μm waveband are higher than those in the 3–5 μm waveband. For LSMO coating, the surface roughness has no significant effect on the emissivity. In the 8–14 μm waveband, variable-emissivity property of LSMO coating remains unchanged before and after ultraviolet irradiation.

Acknowledgements

We are thankful for the financial support provided by the National Natural Science Foundation of China (grant 90505008) and Weaponry Equipment Pre-research Foundation of China.

References

[1] S.S. Kalagi, D.S. Dalavi, R.C. Pawar, et al., J. Alloys Compd. 493 (2010) 335.
[2] J.G. Metts, J.A. Nabity, D.M. Klaus, Adv. Space Res. 47 (2011) 1256.
[3] J. Ye, Y. Lin, Y. Yang, et al., Thin Solid Films 519 (2010) 1578.
[4] A. Piccolo, Energy Buildings 13 (2007) 145.
[5] P.M. Kadam, N.L. Tarwal, P.S. Shinde, et al., J. Alloys Compd. 509 (2011) 1729.
[6] H. Li, K. Xie, Y. Pan, et al., Synth. Met. 159 (2009) 1386.
[7] C. Cai, D. Guan, Y. Wang, J. Alloys Compd. 509 (2011) 909.
[8] K. Sauvet, L. Sauques, A. Rougier, J. Phys. Chem. Solids 71 (2010) 696.
[9] F. Vidal, C. Plesse, P.H. Auberl, Polym. Int. 59 (2010) 313.
[10] I. Valyukh, S. Green, H. Arwin, et al., Sol. Energy Mater. Sol. Cells 94 (2010) 724.
[11] S. Dussan, A. Kumar, J.F. Scott, R.S. Katiyar, Appl. Phys. Lett. 96 (2010) 072904.
[12] S.P. Altintas, A. Amira, N. Mahamdioua, et al., J. Alloys Compd. 509 (2011) 4510.
[13] S. Keshri, L. Joshi, S.S. Rajput, J. Alloys Compd. 509 (2011) 5796.
[14] N. Ibrahim, A.K. Yahya, S.S. Rajput, J. Magn. Magn. Mater. 323 (2011) 2179.
[15] C. Zener, Physiol. Rev. 82 (1951) 403.
[16] P.W. Anderson, H. Hasegawa, Physiol. Rev. 100 (1955) 675.
[17] A.J. Millis, P.B. Littlewood, B.I. Shraiman, Phys. Rev. Lett. 74 (1995) 5144.
[18] J.R. Hattrick-Simpers, K. Wang, L. Cao, et al., J. Alloys Compd. 490 (2010) 42.
[19] K. Shimazaki, S. Tachikawa, A. Ohnishi, et al., Int. J. Thermophys. 22 (2001) 1549.
[20] G. Tang, Y. Yu, Y. Cao, W. Chen, Sol. Energy Mater. Sol. Cells 92 (2008) 1298.
[21] G. Tang, Y. Yu, W. Chen, Y. Cao, J. Alloys Compd. 461 (2008) 486.
[22] G. Tang, Y. Yu, W. Chen, Y. Cao, Mater. Lett. 62 (2008) 2914.
[23] C. Wu, J. Qiu, J. Wang, et al., J. Alloys Compd. 506 (2011) L22.
[24] L.A. Dombrovsky, D. Baillis, Thermal Radiation in Disperse Systems: An Engineering Approach, Begell House Inc., Redding, CT, 2010.
[25] X. Shen, G. Xu, C. Shao, J. Alloys Compd. 499 (2010) 212.